MDPI

Article

Effect of Power Ultrasound on Wettability and Collector-Less Floatability of Chalcopyrite, Pyrite and Quartz

Ahmad Hassanzadeh [1],* , Hamed Gholami [2], Safak Gökhan Özkan [3] , Tomasz Niedoba [4],* and Agnieszka Surowiak [4]

1   Department of Processing, Helmholtz Institute Freiberg for Resource Technology,
    Helmholtz-Zentrum Dresden-Rossendorf, Chemnitzer Straße 40, 09599 Freiberg, Germany
2   Department of Mining and Metallurgical Engineering, Amirkabir University of Technology,
    158754413 Tehran, Iran; hamedgholami@aut.ac.ir
3   Department of Robotics and Intelligent Systems, The Institute of the Graduate Studies in Science
    and Engineering, Turkish-German University, 34820 Beykoz/Istanbul, Turkey; safak.ozkan@tau.edu.tr
4   Department of Environmental Engineering, Faculty of Mining and Geoengineering,
    AGH University of Science and Technology, al. Mickiewicza 30, 30059 Krakow, Poland; asur@agh.edu.pl
*   Correspondence: a.hassanzadeh@gmx.de (A.H.); tniedoba@agh.edu.pl (T.N.); Tel.: +491-7620666711 (A.H.);
    +481-26172056 (T.N.)

Abstract: Numerous studies have addressed the role of ultrasonication on floatability of minerals macroscopically. However, the impact of acoustic waves on the mineral hydrophobicity and its physicochemical aspects were entirely overlooked in the literature. This paper mainly investigates the impact of ultrasonic power and its time on the wettability and floatability of chalcopyrite, pyrite and quartz. For this purpose, contact angle and collectorless microflotation tests were implemented on the ultrasonic-pretreated and non-treated chalcopyrite, pyrite and quartz minerals. The ultrasonic process was carried out by a probe-type ultrasound (Sonopuls, 20 kHz and 60 W) at various ultrasonication time (0.5–30 min) and power (0–180 W) while the dissolved oxygen (DO), liquid temperature, conductivity (CD) and pH were continuously monitored. Comparative assessment of wettabilities in the presence of a constant low-powered (60 W) acoustic pre-treatment uncovered that surface of all three minerals became relatively hydrophilic. Meanwhile, increasing sonication intensity enhanced their hydrophilicities to some extent except for quartz at the highest power-level. This was mainly related to generation of hydroxyl radicals, iron-deficient chalcopyrite and elemental sulfur (for chalcopyrite), formation of OH and H radicals together with H_2O_2 (for pyrite) and creation of SiOH (silanol) groups and hydrogen bond with water dipoles (for quartz). Finally, it was also found that increasing sonication time led to enhancement of liquid temperature and conductivity but diminished pH and degree of dissolved oxygen, which indirectly influenced the mineral wettabilities and floatabilities. Although quartz and pyrite ultrasound-treated micro-flotation recoveries were lower than that of conventional ones, an optimum power-level of 60–90 W was identified for maximizing chalcopyrite recovery.

Keywords: froth flotation; power ultrasound; ultrasonic treatment; chalcopyrite-pyrite-quartz flotation system; hydrophobicity

1. Introduction

Numerous studies have shown the application of ultrasonic frequencies (>20 kHz) *a.k.a* ultra-sonication to mineral beneficiation especially in the interface science [1], biochemistry [2], flotation [3–6] and hydrometallurgy [7,8]. Ultrasonic (US) vibration has been used over four decades as a pre-treatment [9–12] and recently as a simultaneously applied approach [13,14] to flotation in order to improve mineral floatability with a special focus on coal industry [15–19]. Although its application in laboratory has been broadly studied, its fundamental aspects were not adequately reported in the literature.

It is known that the ultrasonic vibration can modify solid-liquid interface and wettability [1]. Theoretically, sonication causes changes on particle surface roughness, dissolved-oxygen concentration, surface oxidation/de-oxidation and an increase in temperature of suspension. However, the role of these modifications on solid-liquid interfaces is unclear, particularly in terms of its application to the froth flotation processes. For instance, Ozun et al. [20] reported that the ultrasonic pre-treatment (60 min, 40 kHz) significantly improved collector-less flotation recovery of oxidized pyrite, however, Cao et al. [21] pointed out that oxidation of the pyrite surface might be assisted and prohibited by ultrasonic treatment (0.3 W/cm^2) strictly depending on the ultra-sonication time. This discrepancy indeed originates from overlooking the impact of dissolved-oxygen concentration, temperature and their interactions induced due to acoustic waves. In this context, Gungoren et al. [22] showed that the positive effect of ultrasound on the quartz-amine flotation recovery was related to the temperature increase during conditioning.

Despite there are several investigations indicated the application of ultrasonic waves during the coal flotation processes [17,18,23–25], there is a considerable lack of study on simultaneous ultrasonic vibration in the mineral flotation processes. To the best of the author's knowledge, it is only limited to colemanite [26], graphite [27], galena [28,29], phosphate [30], magnesite [11], ilmenite [12], copper ore [31–34], copper tailing [35], chalcopyrite [36], scheelite ore [37,38], barite-fluorite-quartz ore [39], lead-zinc-copper ore [40], quartz [13,22] and silica [41,42], calcite and barite [43], talc [44] and feldspar [14] in the literature.

In this scope, Videla et al. [35] applied ultrasound treatment by nine ultrasonic transducers (Clangsonic 2045-68LB P8) at different configurations (i.e., ultrasound conditioning (UC), ultrasound flotation (UF) and flotation and conditioning with ultrasound (FCU)) on El Teniente plant's tailings to enhance the copper recovery. It was indicated that when ultrasound was applied during conditioning and flotation (8 L mechanical Denver cell), copper recovery increased up to 3.5% through cleaning particle surfaces, minimizing slime coatings and facilitating the action of the reagents. Taheri and Lotfalian [36] artificially mixed chalcopyrite and pyrite samples subjecting them to an ultrasonic transmitter (15 min, 280 W and 20 kHz) during the conditioning of micro-flotation experiments. They reported that it is possible to selectively separate chalcopyrite and pyrite using joint aeration and ultrasonic treatment in the light of desorption of metal hydroxide precipitates, as hydrophilic species from the surface of the chalcopyrite by the ultrasonic treatment. Cilek and Ozgen [45] mounted an ultrasonic probe (Bandelin Sonoplus HD 2200, 20 kHz, 0.2 kW), which was located in the froth phase on a 2 L Denver laboratory flotation machine cell. The experimental results showed that the pulp recovery of a chalcopyrite-based ore sample was considerably improved specifically at intermediate and low-level froth depths. However, the froth recovery reduced owing to an increase in bubble coalescences and reduction of available bubble surface area.

Hernández et al. [33] comparatively studied the impact of high-intensity conditioning (HIC) and ultrasonic radiation on floatability of a finely ground Chilean copper ore (El Teniente, Codelco) using a 2.7 L Denver mechanical cell. It was disclosed that the US treatment could provide a promising improvement in copper recovery with 1/3 energy consumption compared to the HIC. Filippov et al. [46] applied an ultrasonic wave to a reactor-separator running with a mixture mineral system of chalcopyrite/quartz. It was shown that chalcopyrite recovery increased by 5–20% with ultrasound treatment. Aldrich and Feng [10] applied 5 L ultrasonic bath (20 kHz and specific power of 2 W/cm^2) to a base-metal sulfide (Merensky ore samples, South Africa) containing the noble metals and liberated platinum group minerals (PGM). The ionic concentration of the ore was reported as Ag = 0.0899, Au = 0.5014, Cu = 0.0516, Ir = 1.1194, Pd = 1.0113, Pt = 0.8227, Rh = 1.0394, Ru = 1.0439 and Pb = 0.0388 ppm). They investigated the role of temperature, solids content, gas input and conditioning time. They found that after ultrasonic excitation, the floatability of the sulfides improved significantly and the silicates were also depressed to some extent. The conditioning time was selected as the most effective factor on flotation rate

constant, selectivity and overall recovery of sulfides. Additionally, they reported in their experiments that there is an optimum temperature (32 °C) where the trade-off between the increase in cavitation bubbles and the attenuation in the intensity of bubble collapse is most favorable to flotation. Aside from these findings for bulk materials, fundamental aspects of ultrasonication in flotation system remain a mystery for researchers.

The motivation and originality of this work are highlighted in two parts. Firstly, the role of sonication time and its power in wettability and floatability is investigated in details, which was overlooked for several decades. Secondly, the impact of liquid temperature, conductivity, pH and dissolved oxygen was studied with a particular focus on physicochemical aspects of acoustic wave for chalcopyrite-pyrite-quartz system.

2. Materials and Methods

2.1. Materials

Thin-layer sections (Figure 1) and highly pure (>95%) mineral crystals of quartz (Qtz, SiO_2, 2.7 g/cm^3), chalcopyrite (Cp, $CuFeS_2$, 4.1 g/cm^3) and pyrite (Py, FeS_2, 5 g/cm^3) were prepared for the contact angle and micro-flotation measurements, respectively. The purities of polished thin sections were qualitatively verified by an optical microscope through their colors and transmission/reflection properties of the minerals. Qtz mainly transmitted the light, while Py and Cp as the opaque minerals both reflected the light.


| (a) | (b) | (c) |
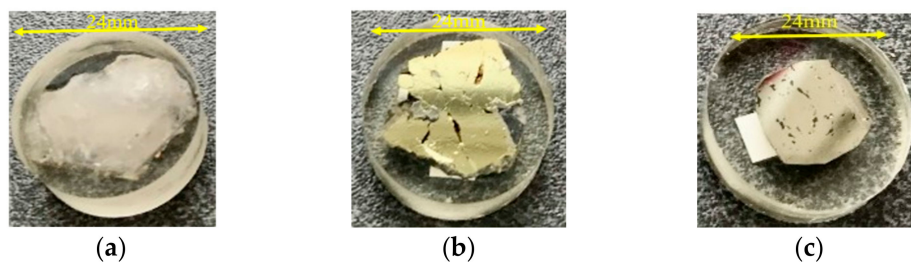
Figure 1. Thin-layer sections of the studied minerals: (**a**) quartz: Qtz, (**b**) chalcopyrite: Cp and (**c**) pyrite: Py for wettability measurements.

These three minerals were selected to represent the key valuable (chalcopyrite) and problematic minerals (pyrite and quartz) typically containing in the sulfide-type copper deposits by imitating possible occurrences in an ore under given ultrasonic treatment.

2.2. Methodology and Apparatus

The pre-treated powder and thin-layer samples were excited by a low-powered ultrasonic source. The drop shape analysis and a modified-Hallimond tube were applied to measure wettability and conduct micro-flotation tests, respectively.

2.2.1. Contact Angle Measurement

Optical contact angle measuring system (OCA 50 series, DataPhysics, Filderstadt, Germany) with an automatic dosing function was utilized for determining mineral wettability characteristics. In the case of Qtz sample, sessile drop approach was applied while the captive bubble method was undertaken for Py and Cp samples due to their natural hydrophobicities. In captive bubble method, instead of placing a drop on the solid as occurred in the sessile drop, a bubble of air was injected beneath a solid, the surface of which was located in the liquid. To reach a reasonable reproducibility level, wettability tests were redounded quadruple and given error propagation were calculated at 95% confidence level.

Prior to any measurement, the mineral surfaces were polished with a DiaPro 1/4 μm diamond suspension on a DP-Nap polishing cloth for 30 sec. Subsequently, the samples were cleaned in a beaker with DI-water into an ultrasonic bath for 5 min. After that, the samples were rinsed with High Performance Liquid Chromatography (HPLC)-grade

ethanol and swiped with a lint-free cloth. To wipe out any potential contaminations on the mineral surface, samples were then washed up triple with Milli-Q water and blow-dried with pressurized air. Detailed information regarding the sample predation and measurement approach was noted elsewhere [47]. The Young-Laplace equation was fitted to calculate the contact angles [48]. It is worth mentioning that prior to the contact angle and micro-flotation tests, a large volume of deionized water was stocked for using all the experiments while its temperature, pH, conductivity and dissolved-oxygen (DO) level were monitored continuously.

2.2.2. Micro-Flotation Tests

Collector-less micro-flotation tests were opted because it allowed us to remove the interaction of chemical reagents on mineral surfaces and better perception of the ultra-sonication role in the mineral surfaces in the absence of surfactants (collector, frother and depressant). Additionally, it has been widely reported in the literature that the acoustic waves improve the binding of collector molecules with the surface of minerals, improve adsorption of chemical agents and later increase their recoverabilities [13,20]. Since this is well-studied in the literature, we focused on collector-less aspect of these minerals which is not adequately addressed.

To determine the flotation recovery of Qtz, Cp and Py, their highly pure mono-minerals were all ground down to the size fraction of $-71 + 56$ μm using a lab roller mill (SFM-14, MTI Corporation, Richmond, CA, USA) operated in a dry environment. This size fraction is the intermediate particle range, which is the most suitable particle spectrum for the flotation experiments [49].

Micro-flotation experiments were performed identically on both ground non-treated and US-pre-treated samples. One gram of the single minerals was added to 10^{-2} M potassium chloride (KCl) as a background electrolyte and aqueous solution while stirring on a magnetic stirrer at 250 rates per minute (rpm). According to the previous study [50], the selected electrolyte allowed a low ionic strength, stabilization of water hydration shells of minerals particularly non-metallic ions by non-paired electrolytes leading to a reduction in the dissolution rate of mineral compared to using pure water. Also, 10^{-2} M KCl provided an equilibrium condition for the suspension. Later, solution pH was adjusted to 9 with a conditioning time of 3–5 min using sodium hydroxide (NaOH) and hydrochloric acid (HCl). NaOH and HCl used for pH adjustment in the micro-flotation tests were supplied by Carl Roth GmbH + Co. KG (Karlsruhe, Germany).

The pH 9 was selected regarding our previous studies [51–53], which showed a requirement for pH $\geq$ 9 to achieve the highest selectivity separation of chalcopyrite and integrate the results of micro-flotation tests with the bulk flotation experiments in an alkaline condition.

After stabilization of pH, the suspension was transferred to a 180 mL volumetric modified-Hallimond tube mounted on a stirrer running in 400 rpm for 3 min to keep the solid well suspended. While the suspension mixed in 700 rpm air flow rate of 20–30 cm^3/min was supplied to the tube and concentrated froth was continuously collected for 1 min. Micro-flotation products were filtered, weighted and later dried in an oven at 50–60 °C overnight. All the experiments were conducted twice and the error propagation was calculated in 95% confidence level. Micro-flotation mass recovery of each single mineral was calculated based on the dry weights using the following equation:

$$R = \frac{C}{F} \times 100 \tag{1}$$

where R (%) is the micro-flotation mass recovery, C (g) and F (g) are dry concentrate and feed masses, respectively.

2.2.3. Ultrasonic Treatments

The ultrasonic treatment process on the highly pure mono-minerals and thin layer sections was performed by a probe-type ultrasound (Bandelin Sonoplus, HD 2200, Germany) at a constant frequency of 20 kHz, with a scalable power level of 30–200 W and probe diameter of 12.7 mm. The effect of sonication power (0, 30, 60, 90, 120 and 180 W) by keeping the time constant (15 s) and its time (0–30 min) at a constant power (60 W) were studied on wettability of all three minerals in detail.

The generator supplied high-frequency electrical energy, which was converted into mechanical vibrations by the transducer. These vibrations were amplified in the amplifier and propagated by the probe in the form of acoustic waves into the liquid medium. It provided intense effects, with a homogeneous and reproducible distribution [54]. It is worth mentioning that commonly used nominal power magnitudes are reported in the present study. Indeed, acoustic power dissipated in the liquid (Pus in W) is related to the power percentage indicated on the ultrasonic generator (P%us in %) using well-known calorimetric method formulated as Pus=0.626 P%us [55]. The AL15 multifunctional instrument (AQUALYTIC, Germany) used for measuring dissolved oxygen (DO) content and liquid conductivity (CD). A digital pH-meter (pH 110, VWR, Germany) was utilized for measuring pH and temperature simultaneously. Both devices were calibrated before being operated in every series of experiments according to the related standards.

3. Results and Discussion

3.1. Mineral Hydrophobicity

3.1.1. Effect of Sonication Time

Figure 2 illustrates the results of Cp, Py and Qtz contact angle measurements with and without the ultrasonic pre-treatment as a function of sonication time at a constant power level of 60 W. The duration of ultra-sonication was varied at 0 (without the US), low (30, 45, 60 and 90 s) and high (10, 20 and 30 min) levels. As seen in Figure 2a–c, surface of all three minerals become hydrophilic by being subjected to the acoustic waves at any time frame.

Figure 2a displays resultant contact angles of fresh and ultrasonic-treated chalcopyrite as a function of sonication time in the absence of any surfactant. As seen, the pure chalcopyrite indicates an average value of 55°, which is the same value presented by An and Zhang [56]. Similar to pyrite (Figure 2b) and quartz (Figure 2c) but with different magnitudes, chalcopyrite becomes hydrophilic by subjecting to the acoustic waves (60 W). In the presence of water and oxygen, chalcopyrite is thermodynamically unstable but its oxidation is rather a slow process. Polarization of solid electrodes changes the surface tension or surface free energy at the solid-liquid interface that leads to the alteration of its angle of wettability [57]. By immersing pure chalcopyrite into an acidic solution (pH less than 6.8), the following reaction takes place proposed by Gardner and Woods in 1979 [58]:

$$CuFeS_{2(s)} \rightarrow CuS_{(s)} + S^0_{(aq)} + Fe^{2+}_{(aq)} + 2e^-. \tag{2}$$
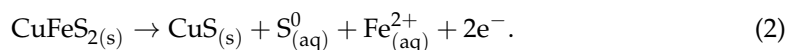
The X-ray photoelectron spectroscopy (XPS) evidence reported by Grano et al. (1997) [59] suggest formation of an iron-deficient chalcopyrite lattice rather than elemental sulfur (Equation (3)).

$$CuFeS_{2(s)} + \frac{3}{4}xO_{2(g)} + \frac{3}{2}xH_2O_{(l)} \rightarrow CuFe_{1-x}S_{2(s)} + xFe(OH)_{3(aq)}. \tag{3}$$

By exposing chalcopyrite to the accusative waves, its surface coated hydrophobic species that is, iron-deficient chalcopyrite (reaction 3) and elemental sulfur (reaction 2) are removed and turns the surface to become more hydrophilic. By increasing the sonication time, surface of chalcopyrite remains hydrophilic. This can be because the chalcopyrite reaches the temperature (47 to 62 °C) required for surface oxidation in 10–30 min. Further, generation of hydroxyl radicals through acoustic waves together with conversion of ferrous

ions (Fe^{2+}) on the chalcopyrite surface to ferric ions (Fe^{3+}) may facilitate the process. Slight dissolution of Cu and Fe ions from the mineral surfaces can be another reason or the mineral might have even disintegrated with an increase in the ultrasound time. Further information regarding the potential of pulp and surface zeta potential of mineral can be useful for profounder understating of its wettability mechanism.

In the case of sonication of pyrite in 30 s at 60 W, its contact angle reduces from an average value of 66° (fresh) to 53° (Figure 2b). The resultant contact angle of non-treated pyrite is in the range of 59–73°, which fits well to the information reported in the literature (68–86°) that examined eight different pyrite samples taken from various mines [60]. The attenuation of pyrite contact angle as a function of sonication time is become more significant at longer ultrasonications (10–30 min). It is known that natural pyrite like other sulfide minerals show hydrophobic properties in anaerobic environment but its surface oxidizes and becomes hydrophilic by exposing to the atmosphere or aqueous media [61]. Such oxidation creates sulfate, iron oxides/hydroxides and an underlying surface-rich layer [62] as follows:

$$FeS_{2(s)} + 8H_2O_{(l)} \rightarrow Fe^{3+}_{(aq)} + 2SO^{2-}_{4(aq)} + 16H^+_{(aq)} + 15e^- \tag{4}$$

$$FeS_{2(s)} \rightarrow Fe^{2+}_{(aq)} + S^0_{(aq)} + 2e^-. \tag{5}$$
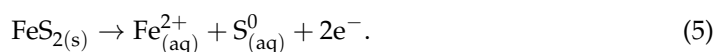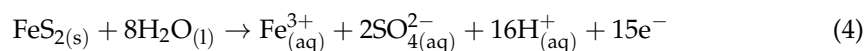
Under the acoustic condition, dissolved gas and water vapour in the cavitation bubble undertake a thermal decomposition leading to the formation of OH and H radicals (reaction 6), which involved in secondary reactions (i.e., reactions 7–10) [15].

$$H_2O \rightarrow \cdot OH + H\cdot \tag{6}$$

$$H\cdot + H_2O \rightarrow H_2 + \cdot OH \tag{7}$$

$$H\cdot + O_2 \rightarrow \cdot HO_2 \tag{8}$$

$$\cdot OH + \cdot OH \rightarrow H_2O_2 \tag{9}$$

$$\cdot HO_2 + \cdot HO_2 \rightarrow H_2O_2 + O_2 \uparrow. \tag{10}$$
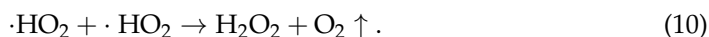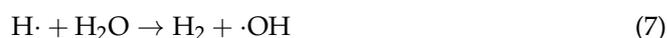
Both products of reaction 10 can oxidize pyrite surface and reduces its hydrophobicity. It was also reported in the literature that hydrogen peroxide (H_2O_2) can be formed by drawn pyrite in water [63], which is a strong oxidizing agent for pyrite, leading to a reduction in its contact angle. Nooshabadi et al. [64] and Cao et al. [21] observed notable concentration of H_2O_2 in pulp during wet-grinding and flotation of pyrite, respectively. Our findings in Figure 4b are in line with the results of Cao et al. [21] who addressed lowering pyrite contact angle to below 31° in the presence of 40 s ultrasonication (0.3 W/cm^2), which was even lower than that of pyrite oxidized in H_2O_2 solution for 2 min. This was related to the chemical effect of ultrasonication. After eliminating initial oxidation products in early stages of sonication, cavitation bubbles are generated at the fresh pyrite surface, which leads to formation of H_2O_2 and oxygen during the process. This is anticipated to further oxidize the pyrite surface and make it more hydrophilic by increasing sonication time.

As seen in Figure 2c, quartz contact angle substantially drops from 12° (non-treated) to 5° on average after irradiating to the acoustic waves for 90 sec. As broadly known, a bare quartz is a hydrophilic mineral with a natural contact angle of around 11–15° [65,66], which is in an absolute agreement with our presented data. Quartz surface has unsatisfied Si and O bonds, which hydrolyze to form SiOH (silanol) groups and in turn create hydrogen bond with water dipoles. Whenever interaction with water to form this hydrated surface is identified, it indicates a hydrophilic surface [67]. One reason to reduction of its hydrophobicity by increasing sonication time is due to the fact that the ultra-sonication can slightly change surface topography of quartz. By increasing its roughness, the apparent contact angle decreases, which are supported by Ulusoy and Yekeler [68] and Chau et al. [48]. In contrast, Gungoren et al. [13] addressed an enhancement in quartz recovery at a low-power

level (30 W) because of an increase in its contact angle (from 52° to 62° in the presence of 10^{-3} M DAH) and slight change of its surface roughness (from 3.70 to 4.24 μm). In this context, Zhu et al. [69] pointed out some inconsistencies of wettability and floatability of quartz in the literature focusing on its roughness property. We believe that surface chemistry aspect of ultrasonication in previously reported works is notably overlooked and further observations consisting surface topography measurements and heterogeneity considering possible chemical and electrochemical reactions on quartz surface can help to clarify these contradictions.
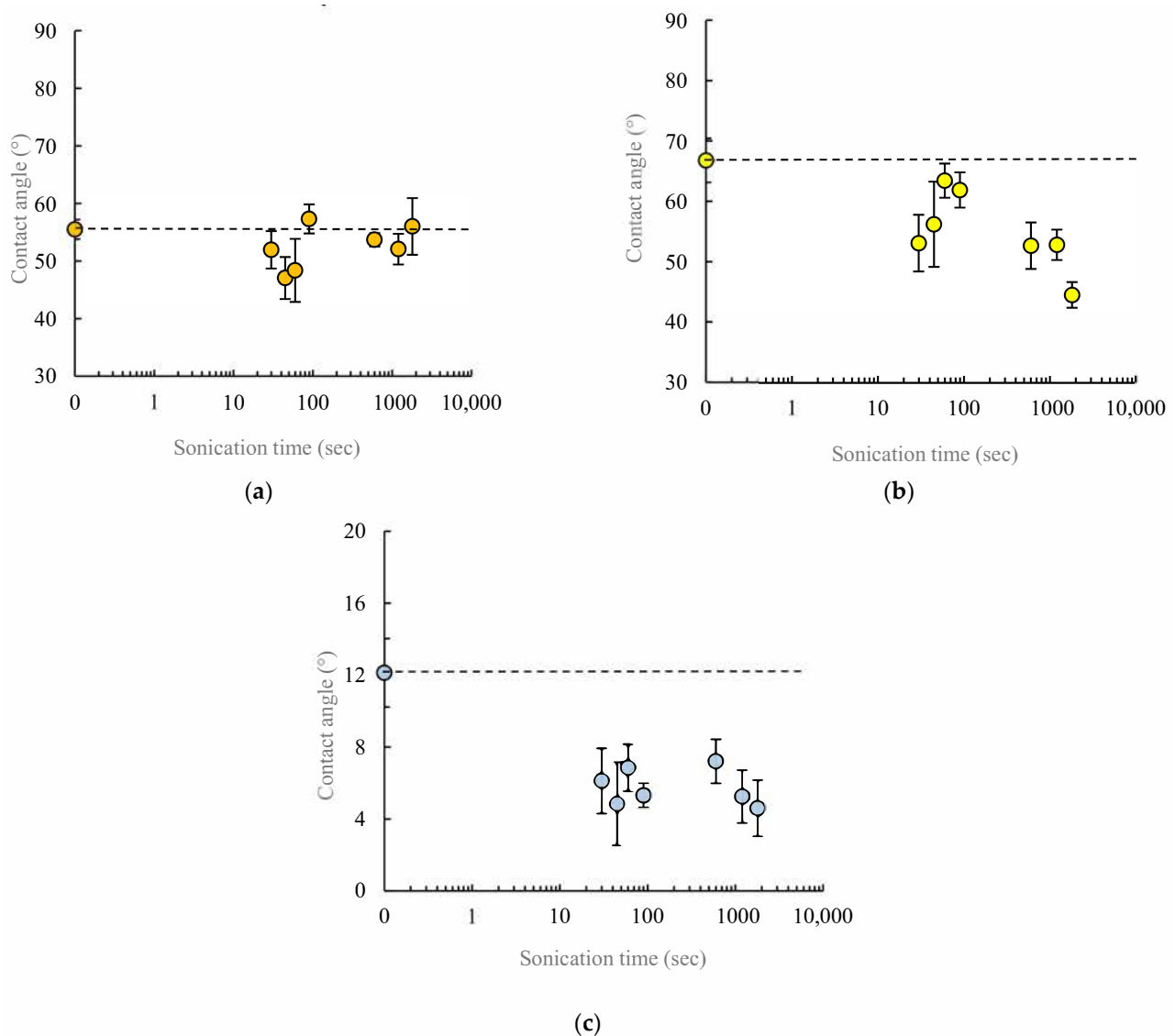

Figure 2. The results obtained from the wettability measurements of (**a**) Cp, (**b**) Py and (**c**) Qtz as a function of sonication time at the power of 60 W.

3.1.2. Effect of Sonication Power

Figure 3 exhibits the impact of ultrasonication power (0 to180 W) on the hydrophobicity of the minerals studied while its duration was constant (15 s). As seen in Figure 3a, surface of chalcopyrite becomes more hydrophilic by increasing sonication power from 0 to 60 W, however, at 60 W < P < 180 W, it does not significantly change. The reason can be contributed to both physical and chemical aspects of sonication power. At power magnitudes lower than 60 W, the ultrasonic intensity is proportional to the amplitude of

vibration of the ultrasonic source and, as such, an increment in the amplitude of vibration leads to an increase in the intensity of vibration. This in turn leads to an increase in the sonochemical effects. At power values >60 W and high amplitude of sonication, rapid deterioration of the ultrasonication results in liquid agitation instead of cavitation and poor transmission of the ultrasound through the liquid media. This probably causes a decrease in contact angle of chalcopyrite by increasing power. In case of pyrite, it seems that the physical impact of sonication is less than its chemical aspects, which can be related to crystallography of the mineral lattice. As noted in Section 3.1.1, in addition to generation of H_2O_2, OH and H radicals can considerably change surface properties of pyrite, which sophisticates its interpretation. In this context, Cao et al. [21] found out that ultrasonication ($0.3 \ W/cm^2 \leq P \leq 0.9 \ W/cm^2$) could result in surface cleaning and further oxidation of both slightly and heavily oxidized pyrite within 40 s. They concluded that the influence of ultrasonication is governed by the time rather than the intensity of ultrasonication.
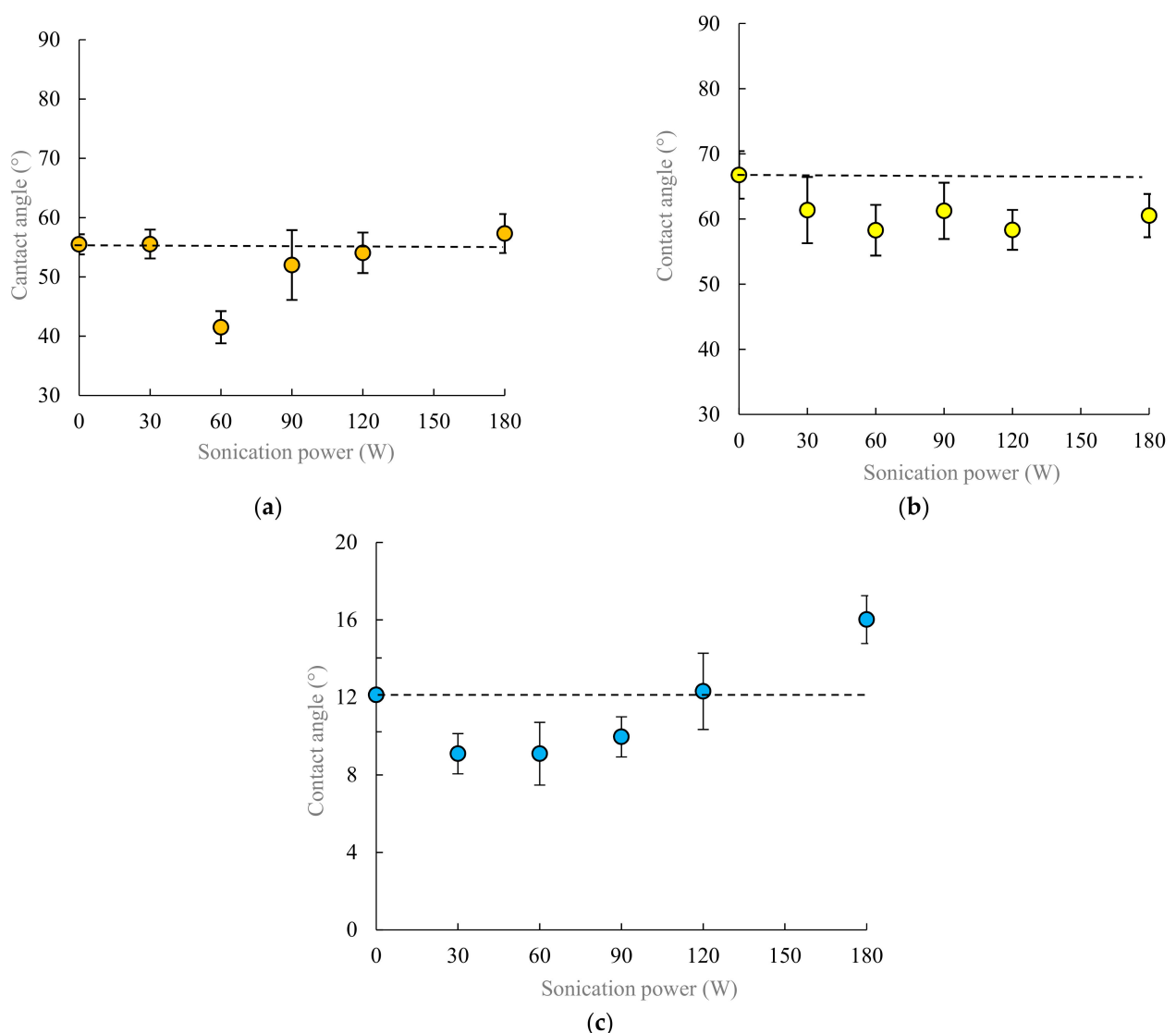

Figure 3. The results of wettability measurements of (**a**) Cp, (**b**) Py and (**c**) Qtz as a function of sonication power at 15 s.

With regard to quartz, as seen in Figure 3c, by increasing the acoustic intensity to 30–90 W, its surface becomes relatively more hydrophilic. While, at the power level of 90 W, the quartz surface has the same wettability as if the non-treated one. It can be concluded from Figure 3a–c that since the minerals studied have different surface and crystallographic characteristics, they behave differently as expose to the acoustic waves. Although the

previous researchers conducted experiments in order to understand the possible effects of ultrasonication power and time for coal [24], quartz [13,22] and pyrite [21] froth flotation separately, the mechanism of ultrasonic intensity is little explored so far. Certainly, further studies are required in future works to perceive the impact of sonication power on minerals.

It is worth mentioning that we considered 60 W as a low ultrasonic power (<200 W) in this work because of the well-known fact that ultrasound waves increase the ambient temperature according to the ultrasounds power and application time (Figure 4a) [70]. As shown in Figure 4, the monitored liquid temperature, pH, liquid conductivity and dissolved oxygen contents in the absence of ultrasonication are almost constant. It is worth noting that these measurements were performed in the absence of minerals/powders meaning any change is indeed reflected to the role of acoustic waves at the corresponding time values.


(a)

(b)

(c)

(d)
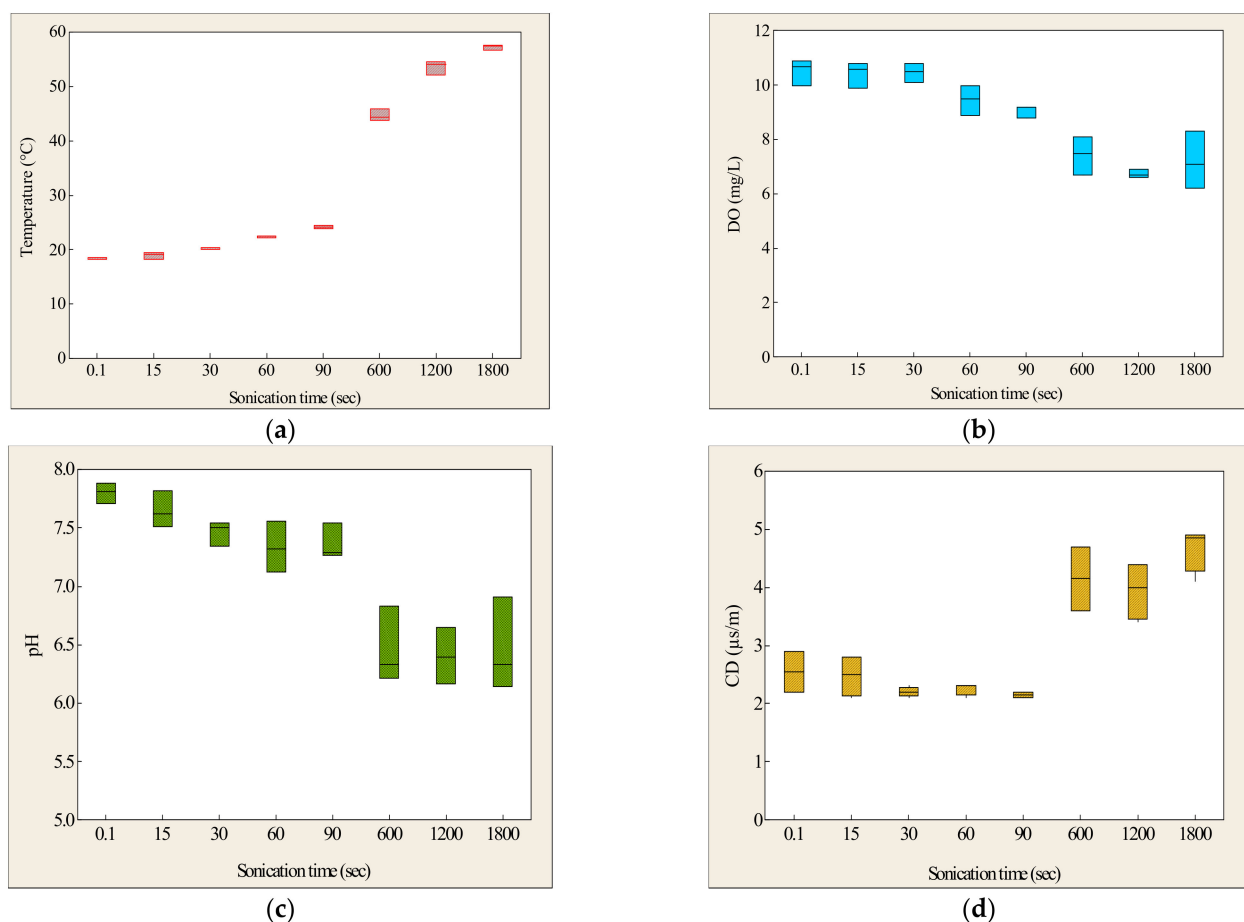
Figure 4. Variation of (**a**) temperature, (**b**) dissolved oxygen (**c**) pH and (**d**) conductivity versus sonication time.

To the best of the author's knowledge, research works reported in the literature entirely overlooked the impact of influential factors (e.g., medium temperature, oxygen solubility, conductivity and pH) and their interconnections involved in sonication studies in the solid-liquid interface of the froth flotation. In Figure 4, we monitored these parameters as a function of acoustic time from 0–30 min, which consequently impacted on the medium and particle/mineral surface properties. Water temperature and its pH during the measurements without the sonication were 21 ± 2.1 °C and 7.5 ± 1.3. According to the results, from 0–1.5 min, the recorded values slightly change, which are more pronounced in longer sonication (>10 min).

Increasing temperature of liquid medium in the presence of acoustic waves because of cavitation and creation of energy which in turn transforms to heat is a well-known phenomenon [70]. It can be seen that water temperature increases from 20.7 °C (0 min) to

24.0 °C (at 1.5 min) and later reaches to 64.1 °C at 30 min sonication. In case of dissolved oxygen content, it is interestingly observed that its magnitude reduces by increasing sonication time particularly at t > 1 min (Figure 4b). However, Kang et al. [15] reported that the nascent oxygen increased in water by ultrasonic conditioning time (0–8 min) (Equation (10)) and it reacted with mineral particles existing in the pulp, which reduced the oxygen content of the pulp. The pH was reported as 7.0 and 7.2 in the absence and presence of acoustic waves, which is absolutely not a notable difference. Whereas, based on the given results shown in Figure 4c, average pH-value decreases with increasing sonication time from 7.8 (non-treated water) to 6.4 (30 min ultrasonication). This is most likely related to the variant concentration of $\cdot OH$ and $\cdot H$ free radicals, which has substantial activity during sonic cavitation (Equations (6)–(8)). In this regard, Giriuniene and Garoka [71] showed that by switching on an ultrasonication device with 34 kHz, pH of a DI-water drops down because the hydrogen ions' concentration in the water increases with time approaches the equilibrium value. This was corresponded to the change of liquid conductivity, which is in line with our results presented in Figure 4c,d. Similar to the temperature, DO level and pH, liquid conductivity slightly changes at low ultrasonication time (t < 1.5 min). However, this variation dramatically rises up from 2.2 µs/m (1.5 min) to 4.9 µs/m (30 min) on average, respectively. This is directly linked to the change of pH and creation of highly reactive radicals ($\cdot OH$ and $\cdot H$), that an enhancement on concentration of ions results in increasing the specific conductivity of electrolyte.

In addition to studying variation of one parameter as a function of acoustic time, one must consider the interactive effective of four factors. For instance, it is widely known that oxygen solubility in water is strongly dependent on liquid temperature and pressure, which decreases at higher temperatures and increases at higher pressure. Therefore, not only the main effect but specifically also interlinked role of four studied factors should be included in application of sonication to the flotation tests. This has not been reported in the previous studies in the literature and highly need further investigations in future works.

3.2. Effect of Sonication Power on Floatability of Mono-Minerals

Figure 5 illustrates the impact of ultrasonication power (in 15 s) on the collector-less micro-flotation mass recoveries obtained for the three minerals at pH 9. As seen in Figure 5a, recoverability of chalcopyrite and quartz in terms of acoustic power is non-linear and there is an optimum domain of sonication power where the chalcopyrite recovery maximizes but the quartz recovery becomes minimized. As known, chalcopyrite is naturally floatable to some extent [72]. The non-treated chalcopyrite recovery is 3.9 ± 1.3% (0 W), which increases by increasing the power-level to 90 W (up to 12.1 ± 1.4%) and later decreases to 6.7 ± 0.5% (at 180 W). Since dissolution rate of chalcopyrite is extremely low [73] and floatation takes place in the absence of any collector, its surface charge characteristic determines the main chemical reactions. Pure chalcopyrite particles react with DI-water in an alkaline pH as given in Equation (11) [60].

$$CuFeS_{2(s)} + 3H_2O_{(aq)} \rightarrow CuS_{(s)} + S^0_{(aq)} + Fe(OH)_{3(aq)} + 3H^+_{(aq)} + 3e^-. \tag{11}$$
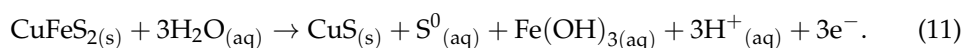
According to Equation (11) and Figure 5, the oxidation product that renders the mineral hydrophobicity is passive layers of either elemental sulfur or polysulfide, depending on the pH and the extent of oxidation. Other than that, it can be seen in the absence of sonication (Figure 5) that chalcopyrite recovery is less than that of quartz, which refers to the initial surface oxidation of its particles. By applying acoustic waves in power-levels lower than 90 W, initially the physical aspect of sonication removes the superficial oxidative layers leading to an improvement in chalcopyrite recovery. Further, generation of surface micron-sized (nano) bubbles through the cavitation phenomenon assists this process, which we discussed it in details in our previous studies [74,75]. However, in higher power-levels (>90 W), particle surfaces probably become oxidized and excessive oxidation produce thiosalts and ultimately sulfates. These ions together with the metal ions may react and re-adsorb as hydrolysis products on the particles creating hydrophilic surfaces. In this

regard, Mao et al., (2020) [76] most recently reported that either lower ultrasonic power (<200 W) or non-treatment was beneficial for improving flotation recovery of coal particles compared to a degassed water, which is in agreement with our findings for chalcopyrite.
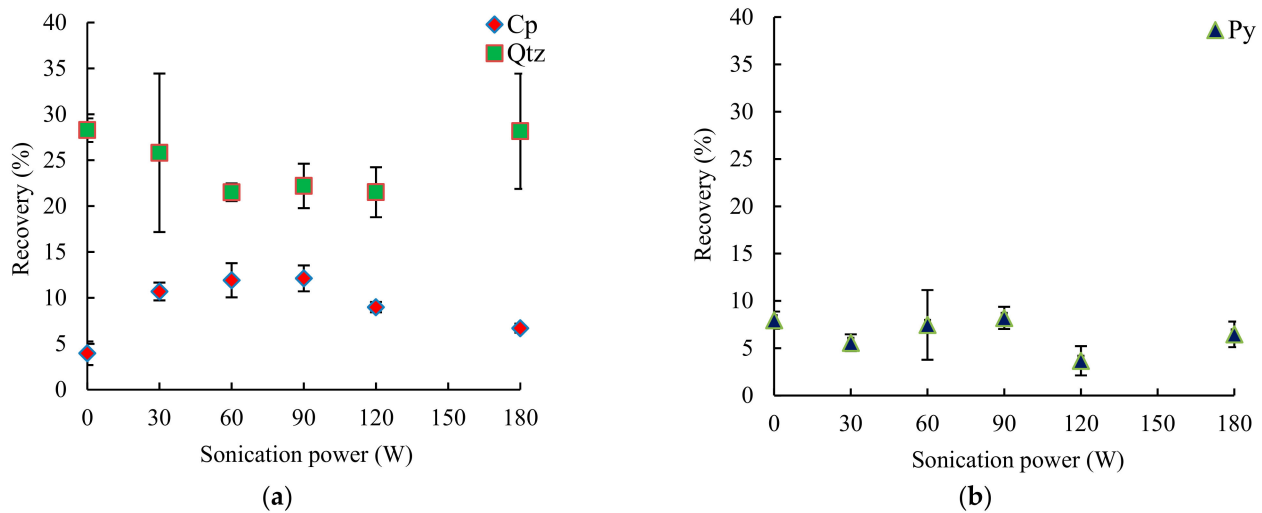

Figure 5. Micro-flotation mass recovery of (**a**) chalcopyrite and quartz and (**b**) pyrite as a function of sonication power at pH = 9, 1 min flotation time and 15 s acoustic pretreatment.

In the case of quartz particles, its recovery first relatively drops from 28.3 $\pm$ 1.3% (non-pretreated) to 22.2 $\pm$ 2.4% by increasing acoustic power to 90 W. Later, its recovery reaches to 28.2 $\pm$ 6.3% under an intensive power-level of 180 W. Reduction of its recovery can be related to formation of SiOH (silanol) groups and creation of hydrogen bond with water dipoles. In this context, Gurpinar et al. [43] investigated the effect of ultrasonic waves on the floatability of calcite, barite and quartz in the case of single and mixture minerals. Although ultrasonication time and power was not reported clearly, mono-mineral flotation experiments of quartz showed that the ultrasonic treatment adversely impacted its floatability about 20%. In another study, Gungoren et al. [13] reported that the interaction of acoustic waves with the collector adsorption led to adverse effect of ultrasonication on quartz recovery at high power levels. Almost the same conclusion was reported for quartz in a sulfide copper ore by Aldrich and Feng [10], where the silicates were depressed to some extent. Creation of rough surfaces can be another reason. Drelich et al. [77] found surface roughness could stabilize a water film if the water contact angle is less than 65–70°, reducing efficiency of particle-bubble attachment. Most recently, Ng et al. [78] conducted a series of experiments and acknowledge that at certain frequencies and above a certain amplitude, acoustic waves improve the apparent flotation rate constant of quartz.

An increase in quartz recovery at higher sonication intensity can be likely referred to slight dissolution of the mineral and generation of surface active ions concerning an increase in temperature and conductivity of the suspension. In this regard, Gungoren et al. [22] pointed out that the temperature played a significant role in increasing quartz recoverability; however, its surface wettability was not presented. We believe further particle surface analyses particularly surface topography and roughness measurements using optical-profilometer and/or atomic force microscopy (AFM) can be helpful for better understanding of this phenomenon.

Figure 5 manifests that pyrite recovery relatively drops down and somewhat remains constant by changing sonication power. Following our results for Py, there is still an argument in the literature whether acoustic vibration has positive or negative impacts on its floatability. In this regard, CaO et al. [21] interestingly showed that ultrasounds either removed oxidation products from pyrite surface or formed H_2O_2 and oxygen, which the former improved its recovery but the latter diminished it. The same contradictory can be found in investigations conducted by Ozun et al. [20] and Kang et al. [15]. It is worth

mentioning that the obtained results were concluded based on two amendments for each experiment. Thus, further repetitions in future works might be essential for acquiring reliable conclusions from statistical point of view.

The results given in Figure 5 justify a possibility of selective flotation in a copper sulfide ore by pre-treating with an ultrasonication and optimization of its power and time. In this regard, several researchers reported a substantial improvement in copper recovery [21,27,28] and a reasonable silicate depression for an ultrasonic-assisted copper ore flotation [10,29]. Thus, by considering the resultant outcomes from all three mineral wettabilities and floatabilities together with the literature works, we examined the ultrasonic-assisted copper porphyry ore at both rougher and re-cleaner stages. The beneficiation process can be also evaluated by means of the methodology presented in our previous works [79–83]. We recently presented the impact of configuration of sonication in four states on batch flotation of copper porphyry ore [31].

4. Conclusions

The present work aimed at studying wettability and floatability of chalcopyrite, pyrite and quartz at un-treated and ultrasound-treated modes. For this purpose, micro-flotation tests and drop shape analysis technique were conducted on mono-minerals and powders of chalcopyrite, pyrite and quartz. Particular focus was given to the role of dissolved-oxygen content, pH, liquid temperature and its conductivity as a function of ultrasonication time (0–30 min).

The results showed that the ultra-sonication at different times altered surface properties in particular mineral/particle hydrophobicities. In the presence of low-powered sonication pre-treatment, surface of the minerals became more hydrophilic. Also, the ultrasonic-assisted mono-mineral floatabilities showed orderly an increase in chalcopyrite but a declination in pyrite and quartz recoveries. It was found that sonication time and power could physically and chemically affect the mineral surface properties. In the studied time values, by prolonging the sonication the minerals became more hydrophilic. In the meantime, liquid temperature and conductivity were increased from 20.7 °C and 2.5 μs/m (non-treated) to 64.1 °C and 4.9 μs/m (30 min and 60 W), respectively. This was corresponded to the cavitation and creation of energy and its conversion to the heat as well as alteration of pH and creation of highly reactive radicals of OH and H. However, solution pH and dissolved oxygen values were both diminished from 7.8 and 10.6 mg/L to 6.4 and 7.1 mg/L, respectively. We concluded that a combination of these four factors can affect the mineral floatability and wettability.

Recovery and hydrophobicity reductions of the ultrasonic-treated quartz were related to the formation of SiOH (silanol) groups, surface topography and creation of hydrogen bond with water dipoles. In case of pyrite, it was linked to oxidation products on its surface, formation of H_2O_2 and oxygen along with OH and H radials, which was a reason for increasing pH of the medium. Generation of nano-bubble sizes and surface cleaning effect of acoustic waves led to higher floatability of ultrasonic-treated chalcopyrite mono-minerals compared to the non-treated one.

Our results suggest that detailed investigations are highly required for dynamic evaluation of mineral surface modification using advanced analytical and surface characterization technique for example, X-ray photoelectron spectroscopy (XPS) and time-of-flight secondary ion mass spectrometry (ToF-SIMS) to profoundly understand the occurring phenomena during the ultrasonic pre-treatment.

5. Future Works

Following the literature studies, reported results and arguments in this work, application of acoustic waves in froth flotation need further insights from both microscopic and macroscopic perspectives. We stressed some crucial ones below:

- most of researcher's attention is drawn to coal treatment while behavior of either sulfide or non-sulfide minerals to sonication has not been explored adequately;

- a comprehensive work is absolutely a must to discover vibrating effect on surface properties such as roughness and its connection to the mineral crystallography which is so far unknown in the literature.
- little attention is given to numerical simulations and analyses of both probe-type and bath ultrasounds in mineral processing. Thus, computational fluid dynamic and its validation with experimental works might help to design significantly efficient equipment.
- compared to the physical impact of ultrasounds in flotation processes, chemical and physicochemical effects have been almost untouched and should be covered in future works.
- although researchers all have addressed a minimum 2% improvement in copper beneficiation, there is a significant lack of industrial report for ultrasounds application in froth flotation.
- synergetic effect of liquid temperature, medium conductivity, pH and gas solubility have been surprisingly overlooked which need to be taken into consideration in future studies.

References

1. Li, B.; Liu, S.; Guo, J.; Zhang, L.; Sun, X. Increase in wettability difference between organic and mineral matter to promote low-rank coal flotation by using ultrasonic treatment. *Appl. Surf. Sci.* **2019**, *481*, 454–459.
2. Vyas, S.; Ting, Y. A review of the application of ultrasound in bioleaching and insights from sonication in (bio)chemical processes. *Resources* **2018**, *7*, 3.
3. Peng, Y.; Mao, Y.; Xia, W.; Li, Y. Ultrasonic flotation cleaning of high-ash lignite and its mechanism. *Fuel* **2018**, *220*, 558–566.
4. Zheng, C.; Ru, Y.; Xu, M.; Zhen, K.; Zhang, H. Effects of ultrasonic pretreatment on the flotation performance and surface properties of coking middlings. *Energy Sources Part A Recovery Util. Environ. Eff.* **2018**, *40*, 734–741.
5. Mao, Y.; Xia, W.; Peng, Y.; Xie, G. Ultrasonic-assisted flotation of fine coal: A review. *Fuel Process. Techol.* **2019**, *195*, 106150.
6. Chen, Y.; Truong, V.N.T.; Bu, X.; Xie, G. A review of effects and applications of ultrasound in mineral flotation. *Ultrason. Sonochem.* **2020**, *60*, 104739. [PubMed]
7. Swamy, K.M.; Rao, K.S.; Narayana, K.L.; Murty, J.S.; Ray, H.S. Application of ultrasound in leaching. *Miner. Process. Extr. Metall. Rev.* **1995**, *14*, 179–192.
8. Luque-García, J.L.; Luque de Castro, M.D. Ultrasound: A powerful tool for leaching. *Trends Anal. Chem.* **2003**, *22*, 41–47.
9. Nicol, S.K.; Engel, M.D.; Teh, K.C. Fine-particle flotation in acoustic field. *Int. J. Min. Process.* **1986**, *17*, 143–150.
10. Aldrich, C.; Feng, D. Effect of ultrasonic preconditioning of pulp on the flotation of sulfide ores. *Miner. Eng.* **1999**, *12*, 701–707.
11. Özkan, S.G. Beneficiation of magnesite slimes with ultrasonic treatment. *Miner. Eng.* **2002**, *15*, 99–101.
12. Shu, K.; Xu, L.; Wu, H.; Fang, S.; Wang, Z.; Xu, Y.; Zhang, Z. Effects of ultrasonic pretreatment on the flotation of ilmenite and collector adsorption. *Miner. Eng.* **2019**, *137*, 124–132.
13. Gungoren, C.; Ozdemir, O.; Wang, S.G.; Özkan, S.G.; Miller, J.D. Effect of ultrasound on bubble-particle interaction in quartz-amine flotation system. *Ultrason. Sonochem.* **2019**, *52*, 446–454. [PubMed]
14. Malayoglu, U.; Özkan, S.G. Effects of ultrasound on desliming prior to feldspar flotation. *Minerals* **2019**, *9*, 784.
15. Kang, W.Z.; Xun, H.X.; Kong, X.H.; Li, M.M. Effects from changes in pulp nature after ultrasonic conditioning on high-sulfur coal flotation. *Miner. Sci. Technol.* **2009**, *19*, 498–502.

16. Ambedkar, B.; Nagarajan, R.; Jayanti, S. Investigation of high-frequency, high intensity ultrasonics for size reduction and washing of coal in aqueous medium. *Ind. Eng. Chem. Res.* **2011**, *50*, 13210–13219.
17. Özkan, S.G. Further investigations on simultaneous ultrasonic coal flotation. *Minerals* **2017**, *7*, 177.
18. Özkan, S.G. A review of simultaneous ultrasound-assisted coal flotation. *J. Miner. Environ.* **2018**, *9*, 679–689.
19. Barma, S.D. Ultrasonic-assisted coal beneficiation: A review. *Ultrason. Sonochem.* **2019**, *50*, 15–35.
20. Ozun, S.; Vaziri Hassas, B.; Miller, J.D. Collectorless flotation of oxidized pyrite. *Colloids Surf. A Physicochem. Eng. Asp.* **2019**, *561*, 349–356.
21. Cao, Q.; Cheng, J.; Feng, Q.; Wen, S.; Luo, B. Surface cleaning and oxidative effects of ultrasonication on the flotation of oxidized pyrite. *Powder Technol.* **2017**, *311*, 390–397. [CrossRef]
22. Gungoren, C.; Ozdemir, O.; Özkan, S.G. Effects of temperature during ultrasonic conditioning in quartz-amine flotation. *Phys. Probl. Miner. Process.* **2017**, *53*, 687–698.
23. Özkan, S.G.; Kuyumcu, H.Z. Investigation of mechanism of ultrasound on coal flotation. *Int. J. Miner. Process.* **2006**, *81*, 201–203. [CrossRef]
24. Özkan, S.G.; Kuyumcu, H.Z. Design of a flotation cell equipped with ultrasound transducers to enhance coal flotation. *Ultrason. Sonochem.* **2007**, *14*, 639–645. [CrossRef] [PubMed]
25. Özkan, S.G. Effects of simultaneous ultrasonic treatment on flotation of hard coal slimes. *Fuel* **2012**, *93*, 576–580. [CrossRef]
26. Özkan, S.G.; Veasey, T.J. Effect of simultaneous ultrasonic treatment on colemanite flotation. In Proceedings of the 6th International Mineral Processing Symposium, Kuşadası, Turkey, 24–26 September 1996; pp. 277–281.
27. Li, C.; Li, X.; Xu, M.; Zhang, H. Effect of ultrasonication on the flotation of fine graphite particles: Nanobubbles or not? *Ultrason. Sonochem.* **2020**, *69*, 105243. [CrossRef]
28. Lu, D.; Chen, L.; Ma, Y.; Zheng, X.; Wang, Y. Effects of ultrasonic pretreatment on the flotation behavior of galena with and without the presence of pyrite. *Physicochem. Probl. Miner. Process.* **2020**, *56*, 611–624.
29. Gungoren, C.; Baktarhan, Y.; Demir, I.; Özkan, S.G. Enhancement of galena-potassium ethyl xanthate flotation system by low power ultrasound. *Trans. Nonfer. Met. Soc. China* **2020**, *30*, 1102–1110. [CrossRef]
30. Hassani, F.; Noaprast, M.; Shafaei Tonkaboni, S.Z. Enhancement of phosphate flotation by ultrasonic pretreatment. *Iran. J. Chem. Eng.* **2019**, *38*, 251–266.
31. Hassanzadeh, A.; Sajjady, S.A.; Gholami, H.; Amini, S.; Özkan, S.G. An improvement on selective separation by applying ultrasound to rougher and re-cleaner stages of copper flotation. *Minerals* **2020**, *10*, 619. [CrossRef]
32. Djendova, S.; Mehandjiski, V. Study of the effects of acoustic vibration conditioning of collector and frother on flotation of sulphide ores. *Int. J. Miner. Process.* **1992**, *34*, 205–217. [CrossRef]
33. Hernández, Y.V.; Garretón, L.G.; Ortega, L.M.; Belmar, R.V. High-power ultrasound as an alternative to high-intensity conditioning in flotation. In Proceedings of the World Congress on Ultrasonics, Paris, France, 7–10 September 2003; pp. 435–438.
34. Cilek, E.C.; Ozgen, S. Effect of ultrasound on separation selectivity and efficiency of flotation. *Miner. Eng.* **2009**, *22*, 1209–1217. [CrossRef]
35. Videla, A.R.; Morales, R.; Saint-Jean, T.; Gaetet, L.; Vargas, Y.; Miller, J.D. Ultrasound treatment on tailings to enhance copper flotation recovery. *Miner. Eng.* **2016**, *99*, 89–95. [CrossRef]
36. Taheri, B.; Loftalian, M. Effect of ultrasonic pre-treatment and aeration on flotation separation of chalcopyrite from pyrite. *Iran. J. Chem. Chem. Eng.* **2018**, *37*, 199–207.
37. Shepeta, E.; Samatova, L. Skarn-scheelite ores beneficiation stimulation using ultrasonic treatment. *E3S Web Conf.* **2018**, *56*, 03009. [CrossRef]
38. Ignatkina, V.A.; Shepeta, E.D.; Sematova, L.A.; Bocharov, V.A. An increase in process characteristics of flotation of low-grade fine-disseminated scheelite ores. *Russ. J. Non Ferrous Met.* **2019**, *60*, 609–616. [CrossRef]
39. Ślączka, A.S. Effects of an ultrasonic field on the flotation selectivity of barite from a barite-fluorite-quartz ore. *Int. J. Miner. Process.* **1987**, *20*, 193–210. [CrossRef]
40. Kurusun, H.; Ulusoy, U. Zinc recovery from a lead–zinc–copper ore by ultrasonically assisted column flotation. *Part. Sci. Technol.* **2015**, *33*, 349–356. [CrossRef]
41. Farmer, A.D.; Collings, A.F.; Jameson, G.J. Effect of ultrasound on surface cleaning of silica particles. *Int. J. Miner. Process.* **2000**, *60*, 101–113. [CrossRef]
42. Haghi, H.; Noaparast, M.; Shafaei Tonkaboni, S.Z.; Mirmohammadi, M. A new experimental approach to improve the quality of low grade silica; The combination of indirect ultrasound irradiation with reverse flotation and magnetic separation. *Minerals* **2016**, *6*, 121. [CrossRef]
43. Gurpinar, G.; Sonmez, E.; Bozkurt, V. Effect of ultrasonic treatment on flotation of calcite, barite and quartz. *Miner. Proc. Extr. Metall.* **2004**, *113*, 91–95. [CrossRef]
44. Feng, D.; Aldrich, C. Effect of ultrasonication on the flotation of talc. *Ind. Eng. Chem. Res.* **2004**, *43*, 4422–4427. [CrossRef]
45. Cilek, E.C.; Ozgen, S. Improvement of the flotation selectivity in a mechanical flotation cell by ultrasound. *Sep. Sci. Technol.* **2010**, *45*, 572–579. [CrossRef]
46. Filippov, L.O.; Matinin, A.S.; Samiguin, V.D.; Filippova, I.V. Effect of ultrasound on flotation kinetics in the reactor-separator. *J. Phys. Conf. Ser.* **2013**, *416*, 1–6. [CrossRef]

47. Babel, B.; Rudolph, M. Characterizing mineral wettabilities on a microscale by colloidal probe atomic force microscopy. *Miner. Eng.* **2018**, *121*, 212–219. [CrossRef]

48. Chau, T.T.; Bruckard, W.J.; Koh, P.T.L.; Nguyen, A.V. A review of factors that affect contact angle and implications for flotation practice. *Adv. Colloid Interface Sci.* **2009**, *150*, 106–115. [CrossRef]

49. Hassanzadeh, A.; Karakaş, F. Recovery improvement of coarse particles by stage addition of reagents in industrial copper flotation circuit. *J. Dispers. Sci. Technol.* **2017**, *38*, 309–316. [CrossRef]

50. Rudolph, M.; Hartmann, R. Specific surface free energy component distributions and flotabilities of mineral microparticles in flotation—An inverse gas chromatography study. *Colloids Surf. A Physicochem. Eng. Asp.* **2017**, *513*, 380–388. [CrossRef]

51. Agheli, S.; Hassanzadeh, A.; Vaziri Hassas, B.; Hasanzadeh, M. Effect of pyrite content of feed and configuration of locked particles on rougher flotation of copper in low and high pyritic ore types. *Int. J. Miner. Sci. Technol.* **2018**, *28*, 167–176. [CrossRef]

52. Azizi, A.; Masdarian, M.; Hassanzadeh, A.; Bahri, Z.; Niedoba, T.; Surowiak, A. Parametric optimization in rougher flotation performance of a sulfidized mixed copper ore. *Minerals* **2020**, *10*, 660. [CrossRef]

53. Azizi, A.; Hassanzadeh, A.; Fadaei, B. Investigating the first-order flotation kinetics models for Sarcheshmeh copper sulfide ore. *Int. J. Miner. Sci. Technol.* **2015**, *25*, 849–854.

54. Costa, J.M.; Neto, A.F.A. Ultrasound-assisted electrodeposition and synthesis of alloys and composite materials: A review. *Ultrason. Sonochem.* **2020**, *68*, 105193. [CrossRef]

55. Laugier, F.; Andriantsiferana, C.; Wilhelm, A.M.; Delmas, H. Ultrasound in gas–liquid systems: Effects on solubility and mass transfer. *Ultrason. Sonochem.* **2008**, *15*, 965–972. [CrossRef] [PubMed]

56. An, D.; Zhang, J. A Study of temperature effect on the xanthate's performance during chalcopyrite flotation. *Minerals* **2020**, *10*, 426. [CrossRef]

57. Chanturiya, V.A.; Vigdergauz, V.E.; Sarkisova, L.M.; Dorofeev, A.I. The hydrophilic-hydrophobic transitions on chalcopyrite: Electrochemical study. *Phys. Probl. Miner. Process.* **2004**, *38*, 65–78.

58. Gardner, J.R.; Woods, R. An electrochemical investigation of the natural flotability of chalcopyrite. *Int. J. Miner. Process.* **1979**, *6*, 1–16. [CrossRef]

59. Grano, S.R.; Sollaart, M.; Skinner, W.; Prestidge, C.A.; Ralston, J. Surface modifications in the chalcopyrite-sulphite ion system. I. Collectorless flotation, XPS and dissolution study. *Int. J. Miner. Process.* **1997**, *50*, 1–26. [CrossRef]

60. Koval, L.; Matysek, D. Evaluation of contact angle on pyrite surface. *Inz. Miner.* **2014**, *34*, 119–125.

61. Tao, D.P.; Li, Y.Q.; Richardson, P.E.; Yoon, R.H. The incipient oxidation of pyrite. *Colloids Surf. A Physicochem. Eng. Asp.* **1994**, *93*, 229–239. [CrossRef]

62. Lowson, R.T. Aqueous oxidation of pyrite by molecular oxygen. *Chem. Rev.* **1982**, *82*, 461–497. [CrossRef]

63. Borda, M.J.; Elsetinow, A.R.; Strongin, D.R.; Schoonen, M.A. A mechanism for the production of hydroxyl radical at surface defect sites on pyrite. *Geochim. Cosmochim. Acta* **2003**, *67*, 935–939. [CrossRef]

64. Nooshabadi, A.J.; Larsson, A.C.; Kota, H.R. Formation of hydrogen peroxide by pyrite and its influence on flotation. *Miner. Eng.* **2013**, *49*, 128–134. [CrossRef]

65. Jańczuk, B.; Chibowski, E.; Białopiotrowicz, T. Interpretation of the contact angle in quartz/organic liquid film-water system. *J. Colloid Interface Sci.* **1984**, *102*, 533–538. [CrossRef]

66. Jańczuk, B.; Chibowski, E.; Białopiotrowicz, T. Time dependence wettability of quartz with water. *Chem. Pap.* **1986**, *40*, 349–356.

67. Wills, B.A.; Finch, J.A. *Wills' Mineral Processing Technology: An Introduction to the Practical Aspects of Ore Treatment and Mineral Recovery*, 8th ed.; Butterworth Heinemann: Burlington, VT, USA, 2015; pp. 381–407.

68. Ulusoy, U.; Yekeler, M. Correlation of the surface roughness of some industrial minerals with their wettability parameters. *Chem. Eng. Process.* **2005**, *44*, 555–563. [CrossRef]

69. Zhu, Z.; Yin, W.; Wang, D.; Sun, H.; Chen, K.; Yang, B. The role of surface roughness in the wettability and floatability of quartz particles. *Appl. Surf. Sci.* **2020**, *527*, 146799. [CrossRef]

70. Suslick, K.S. The Chemical Effects of Ultrasound. *Sci. Am.* **1989**, *2*, 80–86. [CrossRef]

71. Giriûnienė, R.; Garðka, E. The influence of ultrasound on electrical conductivity of water. *Ultragarsas Ultrasound* **1997**, *28*, 25–28.

72. Fuerstenau, M.C.; Sabacky, B.J. On the natural floatability of sulfides. *Int. J. Miner. Process.* **1981**, *8*, 79–84. [CrossRef]

73. Wang, J.; Faraji, F.; Ghahreman, A. Effect of ultrasound on the oxidative copper leaching from chalcopyrite in acidic ferric sulfate media. *Minerals* **2020**, *10*, 1–17. [CrossRef]

74. Nazari, S.; Shafaei, S.Z.; Hassanzadeh, A.; Azizi, A.; Gharabaghi, M.; Ahmadi, R.; Shahbazi, B. Study of effective parameters on generating submicron (nano)-bubbles using the hydrodynamic cavitation. *Phys. Probl. Miner. Process.* **2020**, *56*, 884–904. [CrossRef]

75. Nazari, S.; Hassanzadeh, A. The effect of reagent type on generating bulk sub-micron (nano) bubbles and flotation kinetics of coarse-sized quartz particles. *Powder Technol.* **2020**, *374*, 160–171. [CrossRef]

76. Mao, Y.; Bu, X.; Shao, H.; Zhou, S.; Xie, G. Effect of air dissolved in water on simultaneous ultrasonic-assisted coal flotation. *Energy Sources Part A Recovery Util. Environ. Eff.* **2020**, 1–10. [CrossRef]

77. Drelich, J.; Chibowski, E.; Meng, D.D.; Terpilowski, K. Hydrophilic and superhydrophilic surfaces and materials. *Soft Matter.* **2011**, *21*, 9804–9828. [CrossRef]

78. Ng, C.Y.; Park, H.; Wang, L. The potential of acoustic sound to improve flotation kinetics. *Miner. Eng.* **2020**, *154*, 106413. [CrossRef]

79. Foszcz, D.; Duchnowska, M.; Niedoba, T.; Tumidajski, T. Accuracy of separation parameters resulting errors of chemical analysis, experimental results and data approximation. *Phys. Probl. Miner. Process.* **2016**, *52*, 98–111.

80. Foszcz, D.; Niedoba, T.; Tumidajski, T. A geometric approach to evaluating the results of Polish copper ores beneficiation. *Gospod. Surowcami Miner.* **2018**, *34*, 55–66.

81. Jamróz, D.; Niedoba, T.; Pięta, P.; Surowiak, A. The use of neural networks in combination with evolutionary algorithms to optimize the copper flotation enrichment process. *Appl. Sci.* **2020**, *10*, 3199.

82. Niedoba, T.; Surowiak, A.; Pięta, P. A multidimensional analysis and modelling of flotation process for selected Polish lithological copper ore types. *E3S Web Conf.* **2017**, *18*, 01005. [CrossRef]

83. Pięta, P.; Niedoba, T.; Surowiak, A.; Şahbaz, O.; Karagüzel, C.; Canieren, Ö. Studies of Polish copper ore beneficiation in Jameson cell. *IOP Conf. Ser. Mater. Sci. Eng.* **2018**, *427*, 1–12. [CrossRef]